



# EUROPEAN SOUTHERN OBSERVATORY

Organisation Européenne pour des Recherches Astronomiques dans l'Hémisphère Austral  
Europäische Organisation für astronomische Forschung in der südlichen Hemisphäre

ESO - European Southern Observatory  
Karl-Schwarzschild Str. 2, D-85748 Garching bei München

---

## Very Large Telescope Paranal Science Operations MIDI User Manual

Doc. No. VLT-MAN-ESO-15820-3519

Issue 82, Date 29/02/2008

Prepared ..... Th. Rivinius, S. Morel  
Date Signature

Approved ..... A. Kaufer  
Date Signature

Released ..... O. Hainaut  
Date Signature

This page was intentionally left blank

### Change Record

Issue	Date	Section/Parag. affected	Reason/Initiation/Documents/Remarks
82	29 Feb, 2008	7.1	Updates for P82, brightness requirement for precision visibilities
81	29 Aug, 2007	all	Updates for P81, sensitivities
80	25 May, 2007	1.2, 6.5 8.1.4	Notes on FINITO Note on photometry frames
80	1 March, 2007	All	Corrections in Sect. 1.2, 5, 6.5
79	31 August, 2006	All	Global revision for P79
78	26 June, 2006	All	Corrected again values of off-target guiding distance and limiting magnitude with ATs ; new format ; new paragraph (7.5) on observation constraints.
77	7 December, 2005	6.4	Paragraph on IRIS
Editor: Thomas Rivinius, Sébastien Morel, ESO Paranal Science Operations ; <a href="mailto:triviniu@eso.org">triviniu@eso.org</a>			

# Contents

<b>1</b>	<b>INTRODUCTION</b>	<b>1</b>
1.1	Scope . . . . .	1
1.2	Acknowledgements . . . . .	1
1.3	Glossary . . . . .	1
1.4	Contacts . . . . .	2
<b>2</b>	<b>A FEW WORDS ON INTERFEROMETRY</b>	<b>3</b>
2.1	Introduction . . . . .	3
2.2	How an interferometer works . . . . .	3
2.3	Interferometric observables . . . . .	4
2.4	Visibility estimators . . . . .	4
<b>3</b>	<b>OBSERVING IN THE INFRARED</b>	<b>6</b>
3.1	Atmospheric transmission . . . . .	6
3.2	Background emission . . . . .	6
3.3	Atmospheric turbulence . . . . .	7
3.4	Conclusion . . . . .	8
<b>4</b>	<b>MIDI OVERVIEW</b>	<b>9</b>
4.1	A bit of history . . . . .	9
4.2	Optical Layout . . . . .	9
4.2.1	Cold optics . . . . .	9
4.2.2	Warm optics . . . . .	11
4.2.3	Dispersion . . . . .	11
4.3	Detector . . . . .	11
<b>5</b>	<b>MIDI IN PERIOD 82</b>	<b>13</b>
5.1	Acquisition . . . . .	13
5.2	Beam combination . . . . .	14
5.3	Spectral dispersion . . . . .	14
5.4	Fringe exposure . . . . .	15
5.4.1	Dispersed-Fourier mode . . . . .	15
5.4.2	Field/astrometry mode . . . . .	16
<b>6</b>	<b>THE VLTI ENVIRONMENT IN PERIOD 82</b>	<b>18</b>
6.1	Telescopes and adaptive optics . . . . .	18
6.1.1	The Unit Telescopes and MACAO . . . . .	18
6.1.2	The Auxiliary Telescopes and STRAP . . . . .	18
6.1.3	Chopping . . . . .	19
6.2	Baselines . . . . .	20

6.2.1	UT Baselines . . . . .	20
6.2.2	AT baselines . . . . .	21
6.3	Delay lines . . . . .	21
6.4	IRIS . . . . .	21
6.5	FINITO . . . . .	23
6.6	Organization of VLTI observations . . . . .	23
<b>7</b>	<b>PHASE-1 PROPOSAL PREPARATION WITH MIDI</b>	<b>24</b>
7.1	Target brightness . . . . .	24
7.2	Time of observation . . . . .	25
7.3	Geometry . . . . .	25
7.4	Guaranteed time observation objects . . . . .	25
7.5	Calibrator stars . . . . .	25
7.6	Observation constraints . . . . .	26
<b>8</b>	<b>MIDI OBSERVATIONS</b>	<b>27</b>
8.1	Observation sequence . . . . .	27
8.1.1	Target acquisition . . . . .	27
8.1.2	Fringe search . . . . .	28
8.1.3	Fringe measurement in Fourier mode . . . . .	28
8.1.4	Photometry . . . . .	28
8.2	Total sequence timing . . . . .	29
8.3	The VLT software environment for phase-2 . . . . .	29
8.4	Post-observation process . . . . .	29
8.4.1	Data handling . . . . .	29
8.4.2	The pipeline . . . . .	30
8.4.3	Data distribution . . . . .	30

## List of Figures

1	Principle of beam combination in long baseline interferometry. . . . .	4
2	Mid-Infrared atmospheric transmission . . . . .	6
3	Principle of MIDI optics. For simplicity, some of the mirrors are illustrated as lenses. . . . .	10
4	Lightpath in MIDI cold optics. . . . .	11
5	MIDI warm optics with individual elements labeled. . . . .	12
6	Image of dispersed fringes obtained in laboratory by MIDI with its grism. . . . .	13
7	Dispersed-Fourier mode of MIDI. The white-fringe tracking is no longer used for observations. . . . .	17
8	Field/astrometry mode of MIDI. . . . .	17
9	A unit telescope (left) and an auxiliary telescope (right). . . . .	19
10	The optical path in the VLTI . . . . .	20

11	Layout of VLTI telescope locations. . . . .	22
12	Difference of magnitude between V and H bands, depending on the spectral type.	22

## List of Abbreviations

AT	Auxiliary Telescope
CS	Constraint Set
DIT	Detector Integration Time
DRS	Data Reduction Software
ESO	European Southern Observatory
FOV	Field Of View
FWHM	Full Width at Half Maximum
IRIS	Infra-Red Image Sensor
ISO	Infrared Space Observatory
MACAO	Multi-Application Curvature sensing Adaptive Optics
MIDI	MID-infrared Interferometric instrument
MIR	Mid-InfraRed
OB	Observation Block
OD	Observation Description
OPC	Observation Program Committee
OPD	Optical Path Difference
OPL	Optical Path Length
OS	Observation Software
OT	Observation Toolkit
P2PP	Phase-2 Proposal Preparation
QC	Quality Control
SM	Service Mode
SNR	Signal-to-Noise Ratio
STRAP	System for Tip-tit Removal with Avalanche Photodiodes
TSF	Template Signature File
USD	User Support Department
UT	Unit Telescope
VCM	Variable Curvature Mirror
VLT	Very Large Telescope
VLTI	Very Large Telescope Interferometer
VM	Visitor Mode

# 1 INTRODUCTION

## 1.1 Scope

This document summarizes the features and possibilities of the MID-infrared Interferometric instrument (MIDI) of the VLT, as it will be offered to astronomers for the six-month ESO observation period P82, running from 1 October 2008 to 31 March 2009.

The **bold** font is used in the paragraphs of this document to put emphasis on the important facts regarding MIDI in P82.

## 1.2 Acknowledgements

The editor thanks Olivier Chesneau (Observatoire de la Côte-d'Azur, France) who wrote the very first version of this manual in August 2002, and also contributed to the update by providing us with some important MIDI facts after commissioning runs. The editor also thanks Monika Petr-Gotzens, Andrea Richichi and Markus Wittkowski at ESO-Garching for their comments, as well as Markus Schöller and Andreas Kaufer at ESO-Paranal, and Jean-Gabriel Cuby (formerly at ESO-Paranal).

## 1.3 Glossary

### Constrain Set (CS)

List of requirements for the conditions (sky transparency, baseline...) of the observation that is given inside an **Observation block** (see below) which is only executed under this set of minimum conditions.

### Observation Block (OB)

The smallest schedulable entity for the VLT/VLTI. It consists of a sequence of **templates** (see below). Usually, one Observation Block includes one target acquisition and one or several templates for exposures.

### Observation Description (OD)

Sequence of templates used to specify the observing sequences within one or more OBs.

### Observation Toolkit (OT)

Tool used to create queues of OBs for later scheduling and possible execution.

### Proposal Preparation and Submission (Phase-1)

The phase-1 begins right after the Call-for-Proposal (CfP) and ends at the deadline for CfP. During this period, the potential users are invited to prepare and submit scientific proposals. For more information, see:

<http://www.eso.org/observing/proposals.index.html>

### Phase-2 Proposal Preparation (P2PP)

Once proposals have been approved by the ESO Observation Program Committee (OPC), users are notified and the phase-2 begins. In this phase, users are requested to prepare their actual observations in the form of OBs, and to submit them electronically (in case of service mode). The software tool used to build OBs is called the P2PP tool. It is distributed by ESO, and can be installed on the personal computer of the user. See:

<http://www.eso.org/observing/p2pp>.

**Service Mode (SM)**

In service mode (opposite of the “visitor mode”, see below), the observations are carried out by the ESO Paranal Science Operation (PSO) staff. Observations can be done at any time during the period, depending on the CS given by the user. OBs are put into a queue schedule in OT which later sends OBs to the instrument.

**Template**

An elementary sequence of operations to be executed by the observation software (OS) of the instrument. The OS dispatches commands written in templates not only to instrument modules that control the detector and motors, but also to the telescopes and VLTI subsystems.

**Template signature file (TSF)**

The file which contains input parameters for a template. Some of these parameters can be set by the user.

**Visitor Mode (VM)**

The classical observation mode. The user is on-the-site to supervise his/her program execution.

## 1.4 Contacts

The authors hope that this manual will help to get acquainted with the MIDI instrument before writing proposals, especially to scientists who are not used to interferometric observations. This manual is continually evolving and needs to be improved according to the needs of observers. If you have any question or suggestion, please contact the ESO User Support Department (<http://www.eso.org/org/dmd/usg/index.html>, email: [usd-help@eso.org](mailto:usd-help@eso.org)). The web page dedicated to the MIDI instrument is accessible at the following URL:

<http://www.eso.org/instruments/midi/>



## 2 A FEW WORDS ON INTERFEROMETRY

### 2.1 Introduction

This section gives a short summary and a reminder of the principles of interferometry. Astronomers interested in using the VLTI and MIDI, but who are not familiar with interferometry yet, can get tutorials from the following links:

- <http://www.sc.eso.org/santiago/science/interf2002.html> (proceedings of ESO-Chile Interferometry Week 2002).
- <http://olbin.jpl.nasa.gov/intro/index.html> (Optical Long Baseline Interferometry News tutorials).
- <http://www.eso.org/projects/vlti/general> (VLTI general description and tutorials).
- <http://www.mariotti.fr/obsvlti/obsvlti-book.html> (proceedings of EuroWinter school “Observing with the VLTI”).
- [http://www.mpia-hd.mpg.de/FRINGE/tutorials/01/tutorial\\_01.html](http://www.mpia-hd.mpg.de/FRINGE/tutorials/01/tutorial_01.html) (tutorial in German).

### 2.2 How an interferometer works

An optical interferometer samples the wavefronts of light emitted by a remote target. Sampling is performed at two or more separate locations (see Fig. 10 and 11 for the case of the VLTI). The interferometer recombines the sampled wavefronts to produce interference fringes. In the MIDI context, the interferometer uses two telescopes as light collectors. The telescopes are separated on the ground by a “baseline” vector. The wavefronts add constructively or destructively, depending on the path difference between the wavefronts, and produce a fringe pattern that appears as bright and dark bands, with the bright bands being brighter than the sum of intensities in the two separate wavefronts. A pathlength change in one arm of the interferometer by a fraction of a wavelength causes the fringes to move. If the beams from the telescopes are combined at a (small) angle, the fringes consist of a spatially modulated pattern on the detector. If the two beams are superimposed coaxially, as in the case of MIDI, the fringes show a temporal modulation of the signal when scanning the optical path difference (OPD) between the two beams.

The angular resolution that the interferometer can achieve depends on the wavelength of observation, and on the length of the projected baseline (the projected baseline vector is the projection of the on-ground baseline vector onto a plane perpendicular to the line-of-sight. The projected baseline changes over the night because of Earth rotation). The smallest angular separation that can be resolved is proportional to the quantity  $\lambda/B$ , where  $\lambda$  is the wavelength of the observation and  $B$  is the projected baseline of the interferometer. This is equivalent to the expression for diffraction-limited spatial resolution in single telescope observations, where  $B$  would be the telescope diameter.

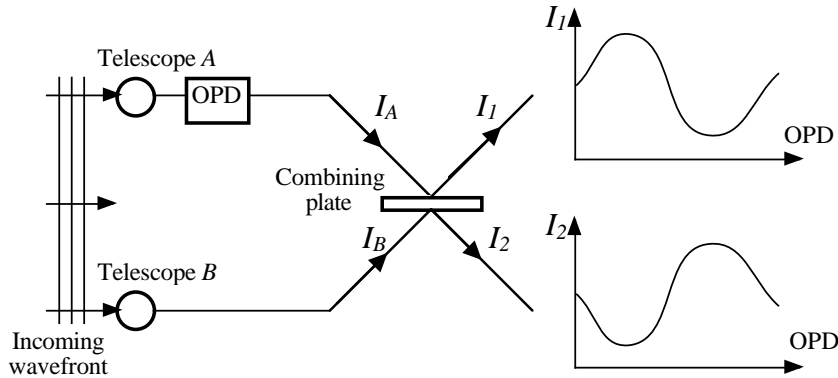


Figure 1: Principle of beam combination in long baseline interferometry.

### 2.3 Interferometric observables

An interferometer measures the coherence between the interfering light beams. The primary observable, at a given wavelength  $\lambda$ , is the complex visibility  $\Gamma = V e^{i\phi} = \hat{O}(u, v)$ . In this expression,  $\hat{O}(u, v)$  is the Fourier transform of the object brightness angular distribution  $O(x, y)$ . The sampled point in the Fourier plane is  $(u = B_x/\lambda, v = B_y/\lambda)$ .  $(B_x, B_y)$  are the coordinates of the projected baseline.

$V$  corresponds to the “visibility”  $(I_{max} - I_{min})/(I_{max} + I_{min})$  of the fringes, its phase  $\phi$  is related to their position.

The visibility can be observed either as the fringe contrast in an image plane or by modulating the internal delay and detecting the consequent temporal variations of the intensity, as has always to be done in the case of coaxial beam combination. This latter mode is used in the MIDI instrument. In this case, the light from two telescopes A and B is combined by a half-transparent plate, and the combiner has two output channels 1 and 2 (Fig. 1). The total observed intensity is ideally given by:

$$\begin{aligned} I_1 &= I_{A1} + I_{B1} + 2V\sqrt{I_{A1}I_{B1}}\sin(2\pi\text{OPD}/\lambda + \phi) \\ I_2 &= I_{A2} + I_{B2} - 2V\sqrt{I_{A2}I_{B2}}\sin(2\pi\text{OPD}/\lambda + \phi) \end{aligned}$$

where  $I_1$  and  $I_2$  are the intensities from the two outputs of the combiner,  $I_{xy}$  the intensity from telescope  $x$  mixed for the channel  $y$  of the combiner, and OPD the path difference introduced by the atmospheric turbulence and by the optomechanical modulator (used to produce interferograms).

### 2.4 Visibility estimators

Due to atmospheric fluctuations (see Sect. 3.3), the fringe pattern to be observed is often in rapid motion, and the phase  $\phi$  of the complex visibility  $\Gamma$  cannot be estimated. It is often better to work with the square of the visibility  $V^2$  rather than  $V$  itself, because  $V^2$  estimators are less affected by the smearing of the moving fringe pattern. Averaging the squared visibility introduces a noise bias which however can be taken into account properly.

Performing a spectral dispersion of the output of a two-element pupil plane interferometer produces the so-called channelled spectrum (i.e., a fringe-modulated spectrum):

$$I(\sigma) = I_0(\sigma)[1 + V(\sigma) \cos(2\pi\text{OPD}\sigma) + \phi(\sigma)]$$

Here,  $\sigma$  is the wave number ( $1/\lambda$ ),  $I_0(\sigma)$  the spectrum of the light target and OPD, the total delay between the light path of the two telescopes. Note that the above equation corresponds to an ideal case for which no atmospheric turbulence would cause OPD fluctuation (see Sect. 3.3), and the incoming beams have the same intensity.

From this equation, we see that fringes with period  $\Delta\sigma = 1/\text{OPD}$  appear in the channelled spectrum, provided that  $I_0(\sigma)$  and  $\Gamma(\sigma)$  do not vary strongly with wavelength.

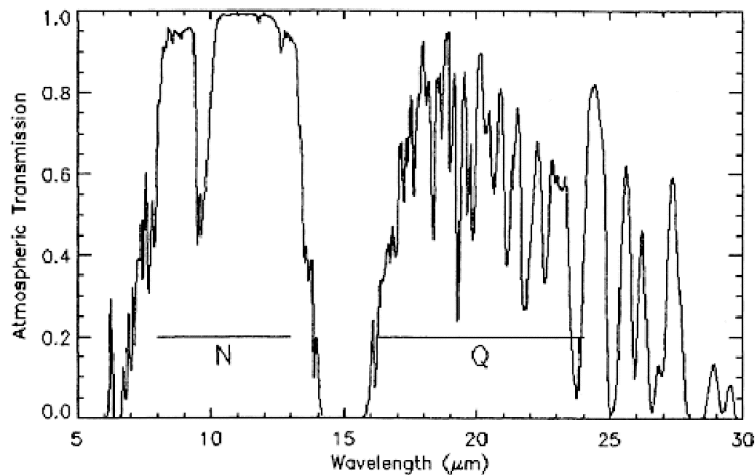


Figure 2: Mid-Infrared atmospheric transmission

### 3 OBSERVING IN THE INFRARED

Interferometric observations strongly depend on the turbulence properties of the terrestrial atmosphere. Observing in the MIR implies additional constraints which are not encountered in optical observations.

#### 3.1 Atmospheric transmission

The thermal infrared (8 to 25  $\mu\text{m}$ ) atmospheric transmission is dominated by aerosol particles and by various molecular species, including  $\text{O}_3$  (9.6  $\mu\text{m}$ ),  $\text{CO}_2$  (14  $\mu\text{m}$ ), and  $\text{H}_2\text{O}$  ( $\leq 7 \mu\text{m}$ ), which absorb large parts of the infrared spectrum. Some of these components are constant for many hours at a time and over the whole sky, others may be variable on quite short time-scales or over short distances in the sky. Ground based mid-infrared observations can only be made in two atmospheric transparency “windows”, the N-band (wavelengths between 7.5 and 14  $\mu\text{m}$ ) and the Q-band (16 to 28  $\mu\text{m}$ ), but even in these windows the atmospheric absorption and radiation are a major disturbance. Nevertheless, new detector technology and the extremely dry mountain top of Cerro Paranal can improve the data quality. Transmission spectra are shown in Fig. 2.

#### 3.2 Background emission

The atmosphere and telescope thermal radiation causes a high background that makes the observation of faint astronomical targets difficult. It is not unusual to observe objects which are thousands of times fainter than the sky. The mid-IR (8 to 15  $\mu\text{m}$ ) sky background is primarily due to thermal emission from the atmosphere i.e. it is equivalent to  $(1 - \text{transmission})$  multiplied by a blackbody spectrum at a temperature of about 250K. The transmission (and therefore the emission) varies with atmospheric water vapor content and air mass.

On MIDI, the thermal background is dominated by 27 reflections (when the UTs are used, or 24 when the ATs are used) in the optical train at ambient temperature, which in combination give a 35% reflection and almost radiate like a blackbody. The thermal background therefore

is dependent on the sky and interferometer temperature (lower in winter for instance) and also on possible dust particles on the numerous mirrors used to relay the beams.

Under these conditions, it has become a standard procedure to observe the target (together with the inevitable sky) and subtract from it an estimate of this sky background obtained by fast switching between target and an empty sky position. The method used with MIDI to deal with this correction is called “chopping”. The characteristic time of such a correction is dependent on the sky variability (which is fast), and on the weather. Sky subtraction has the additional advantage that detector artifacts are removed.

In interferometric setup without the photometric channels, chopping is not employed. To cancel out the background, we rely on the fact that between the interferometric channels of MIDI, the background is almost totally correlated, whereas the interferometric signals are in phase opposition. Subtracting in each detector frame the area illuminated by one interferometric channel from the area illuminated by the other will therefore cancel out the thermal background in the frame.

### 3.3 Atmospheric turbulence

Atmospheric turbulence is a major contributor to the difficulty of optical and infrared interferometry from the ground. Rapid atmospheric variations of the OPD between the two arms of an optical or infrared interferometer, if uncorrected, will cause a smearing of the fringe pattern and a strong decorrelation of the observed signals. The correlation time of the atmosphere is milliseconds in the visible and increases to hundreds of milliseconds in the mid-IR.

“Seeing” is the historical term for the fact that the image produced by a telescope, which is larger than approximately ten centimeters (in optical), is not as sharp as one would expect from its size and optical quality, but is fuzzy. The fuzziness changes with time and weather conditions. A short exposure (milliseconds) of such an image reveals a large number of “speckles”. These speckles move around, disappear and reappear on short time-scales. The speckle image is in fact a result of interference between wavefronts of randomly appearing, moving, and disappearing sub-apertures. These sub-apertures are defined by the atmospheric turbulence “bubbles” in the first few tens to hundreds of meters above the telescope.

The sensitivity of interferometers strongly depends on the seeing, i.e. on the Fried parameter, defined as follows: the resolution of seeing-limited images obtained through an atmosphere with turbulence characterized by a Fried parameter  $r_0$  is the same as the resolution of diffraction-limited images taken with a telescope of diameter  $r_0$ . Observations with telescopes much larger than  $r_0$  are seeing-limited, whereas observations with telescopes smaller than  $r_0$  are essentially diffraction-limited. The scaling of  $r_0$  with wavelength is favorable for MIDI since:

$$r_0 \propto \lambda^{\frac{6}{5}}$$

which at 10  $\mu\text{m}$  and for a 0.8-arcsec seeing in the visible leads to  $r_0 = 4.6$  m. It is therefore much easier to achieve diffraction-limited performance at longer wavelengths, and simple tip-tilt correction already will give correct results with large apertures. An interferometer correctly works only if the wavefronts from the individual telescopes are coherent (i.e., have phase variances not larger than  $\approx 1$  rad<sup>2</sup>).

Scintillation is another consequence of inhomogeneities in the atmosphere at altitudes of some kilometers. Phase gradients due to the pressure gradients of the turbulent air cause mild deflections of the direction of travel of the wavefront. The cross section of the resulting cone of rays, intercepted by the telescope pupil, is at any time brighter or fainter than the

average intensity (the “cylinder of rays” that would ideally feed each telescope in absence of turbulence). Scintillation is less important in the mid-infrared where fluctuations of sky emission (“sky noise”) dominate.

### **3.4 Conclusion**

These observational difficulties, mostly resulting from high background variations, have led to the development of specific observation techniques. These techniques are included in the templates (see Sect. 1.4) that are used to control MIDI and the telescope. The templates are extensively described in the template manual, available from the MIDI webpage at beginning of phase-2 proposal preparation for P82.

## 4 MIDI OVERVIEW

### 4.1 A bit of history

MIDI belongs to the first generation of VLTI instruments. Conceptual studies for a VLTI mid-infrared instrument started in 1997. The Final Design Review of MIDI was passed in early 2000 for the hardware, and mid-2001 for the software. The integration took place at the Max-Planck Institut für Astronomie, Heidelberg (Germany). After Preliminary Acceptance in Europe in September 2002, MIDI was shipped to Paranal and re-assembled there in November 2002, where it obtained its first fringes with the UTs on the 12 December 2002. Since 1 September 2003, MIDI is offered to the worldwide community of astronomers, for observations in service mode or in visitor mode.

The MIDI consortium, who built and commissioned MIDI, consists of several european institutes: Max Planck Institut für Astronomie, Heidelberg (Germany) ; Netherlands Graduate School for Astronomy (NOVA), Leiden (The Netherlands) ; Department of Astronomy, Leiden Observatory (The Netherlands) ; Kapteyn Astronomical Institute, Groningen (The Netherlands) ; Astronomical Institute, Utrecht University (The Netherlands) ; Astronomical Institute, University of Amsterdam (The Netherlands) ; Netherlands Foundation for Research in Astronomy, Dwingeloo (The Netherlands) ; Space Research Organization Netherland, Utrecht and Groningen (The Netherlands) ; Thüringer Landessternwarte, Tautenburg (Germany) ; Kiepenheuer-Institut für Sonnenphysik, Freiburg (Germany) ; Observatoire de Paris-Meudon, Meudon (France) ; Observatoire de la Côte d'Azur, Nice (France).

### 4.2 Optical Layout

Inside MIDI, the beam combination occurs in a plane close to the re-imaged pupil, and the signal is detected in an image plane (infinity).

MIDI in the interferometric laboratory is composed by two main parts: the warm optics on the MIDI table and the cold optics in the cryostat. In addition, in the adjacent Combined Coudé Laboratory, are located an infrared CO<sub>2</sub> laser (used for calibration measurements), the control electronics and the cooling system.

#### 4.2.1 Cold optics

Since radiation at 10  $\mu\text{m}$  is dominated by thermal emission from the environment, most of the instrument optics has to be in a cryostat and to be cooled to cryogenic temperatures (6 K to 12 K for the detector,  $40\pm 5$  K for the cold bench, 77 K for the outer radiation shield).

In the cryostat, the elements of the cold optics appear in the following sequence along the beams:

1. Shutter
2. Cold pupil stops
3. First off-axis paraboloids (M1)
4. Diaphragms in intermediate focus (spatial filters)

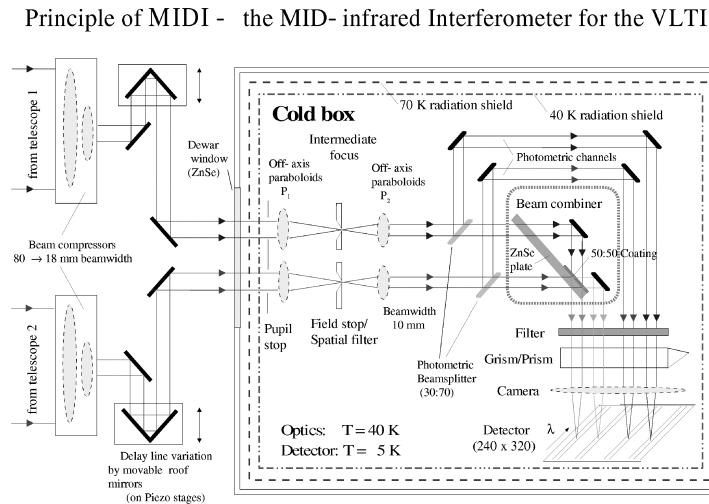


Figure 3: Principle of MIDI optics. For simplicity, some of the mirrors are illustrated as lenses.

5. Second off-axis paraboloids (M2)
6. Folding flat mirror (M3)
7. Photometric beam splitter plates
8. Folding flat mirrors (for one of the photometric channels) (M4 and M5)
9. Beam combiner (beam combiner plate, M6 and M7)
10. Filters
11. Dispersive elements (prism, grism)
12. Cameras
13. Detector

The core of the cold optics is formed by the beam combiner. It consists of a half-transparent plate on which the telescope beams are superimposed with nominally 50% of beam A being transmitted and nominally 50% of beam B being reflected. The remaining light, 50% reflection of beam A and 50% transmission of beam B, is superimposed too, and directed towards the detector thanks to an extra mirror. In addition, the cold optics offers the possibility to extract a signal from the beams before combination (by the mean of cold optics beamsplitters), in order to get the photometric information (see Fig. 4). The intensity extracted by the “photometric” beamsplitters for each beam is around 30% of the incoming intensity.

MIDI has two focusing mechanisms: the first one actuates the M1 mirrors to focus the beams on the spectroscopy slits (if dispersion is used) or on future spatial filters, and the second one translates the detector plane to bring it at the focus of the “camera” (germanium set of lenses). Baffling within the instrument is mainly done by a cold pupil stop just downstream of the entrance window of the cryostat.



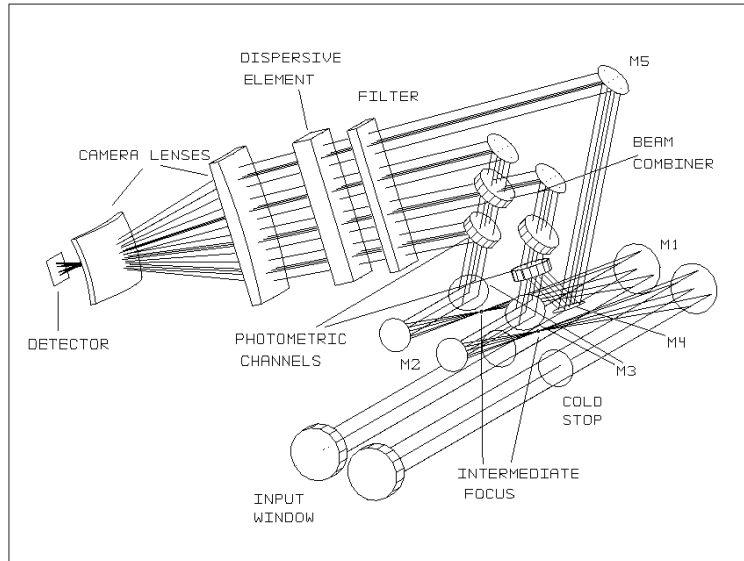


Figure 4: Lightpath in MIDI cold optics.

#### 4.2.2 Warm optics

OPD modulation is performed in the ambient-temperature laboratory environment. An overview on this so-called “warm optics” is given in Fig. 5. As said above, the degree of coherence of the light target (i.e. the object visibility at the actual baseline setting) is determined by stepping the internal OPD rapidly over at least one wavelength within a time when the fringe has not moved more than  $1 \mu\text{m}$  on the average ( $t < 0.1\text{s}$ ). This operation is performed by two dihedral mirrors mounted on piezo translators (DLA and DLB, one for each arm). One piezo is used for OPD modulation. A translation stage underneath one of them (DLA) allows to change the internal OPD by a larger amount.

As sketched by Fig. 5, the warm optics bench also includes ancillary devices for calibration and alignment that can be inserted in the optical path. These devices are beamsplitter and feeding optics for a  $\text{CO}_2$  test laser ( $\lambda=10.6 \mu\text{m}$ ), spatially-incoherent blackbody target, and alignment target plates.

#### 4.2.3 Dispersion

MIDI has a spectroscopic mode based on either a NaCl prism or a KRS5 grism, that are used along with beam combination. The interest of such a mode, besides the possibility to measure fringe visibility for different spectral channels in the N-band, is explained in Sect. 5.3.

### 4.3 Detector

The detector is a  $320 \times 240$ -pixel Raytheon Si:As Impurity Band Conduction (IBC) array (also called “BIB”, blocked impurity band), with the following characteristics:

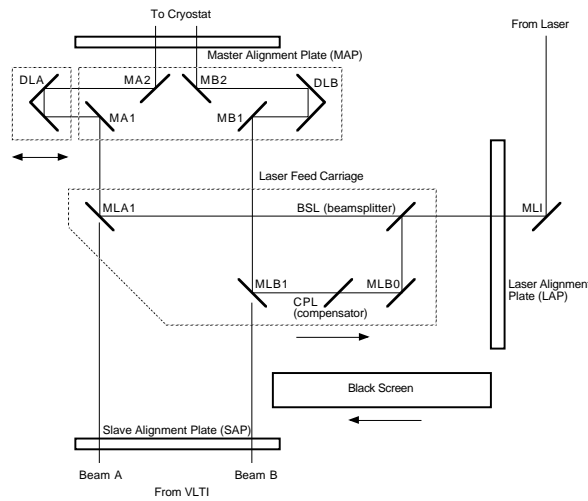


Figure 5: MIDI warm optics with individual elements labeled.

Array dimensions	$320 \times 240$
Pixel Size	$50 \mu m \times 50 \mu m$
Peak Quantum efficiency	34%
Dark current	$10^4 \bar{e}/\text{pix}/\text{s}$ at 10 K
Operating temperature	4-12 K
Well capacity	$1.1e7 \bar{e}$
RON	$\approx 800\bar{e}$

The standard operating mode of the detector is called “Integrate-Then-Read” (ITR). In this mode (“snapshot” mode), before the start of integration, a reset is performed simultaneously on the whole chip and further accumulation of signal is stopped by a bias voltage at the end of integration. The frame rate in “snapshot” mode is determined by the sum of the integration time and the readout time. On the other hand, ITR mode allows to select an integration as short as 0.2 ms per frame. The minimum integration time is given by the time needed to propagate the reset signal. The time required to readout a full frame in ITR mode is about 6 ms.

However, in many cases there is no need to read out the full detector array: it may be advantageous to use sub-array readout (windowing). Windowing of the detector by line selection reduces the time needed for readout. Windowing by software by column selection after readout reduces the amount of data to be processed in the downstream steps of data handling.

Fig. 6 shows the type of data that is collected by MIDI if a dispersive element is inserted in the optical path after the beam recombination: dispersed fringes with phase opposition from the two recombined beams, in the image plane.

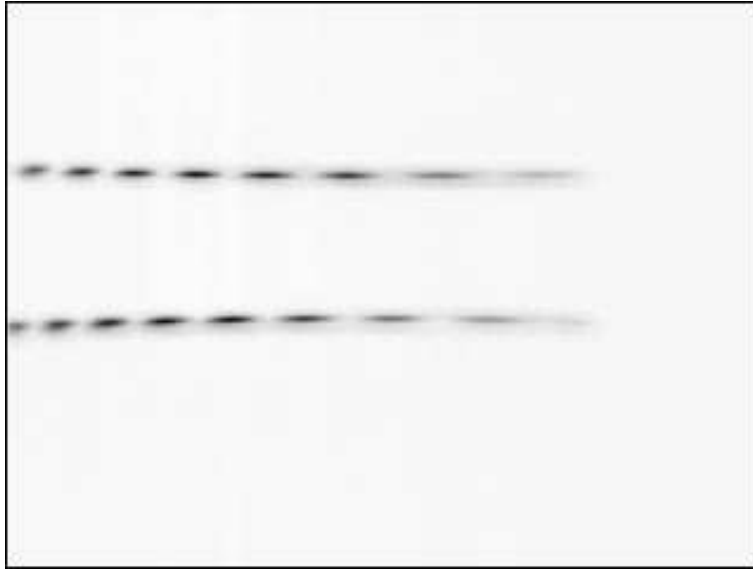


Figure 6: Image of dispersed fringes obtained in laboratory by MIDI with its grism.

## 5 MIDI IN PERIOD 82

MIDI combines most of the aspects that usually exist independently in several astronomical instruments. It involves visibility measurements (interferometry), spectral dispersion (spectroscopy), imaging with a detector array (imaging) and background level plus fluctuation measurement (thermal infrared imaging techniques). Hence, MIDI in its final configuration will offer a large possibility of setups selectable by the user.

**For P82, the available setups consist of:**

- **Acquisition:** imaging mode, several spectral filters available.
- **Beam combination:** “HIGH\_SENS” (high-sensitivity): no simultaneous photometric channel), or “SCI\_PHOT” (science with photometry): simultaneous photometric channels.
- **Fringe type:** dispersed (normal) or white (fringe/astrometry mode, VM only).
- **Spectral mode:** prism or grism, with 200- $\mu\text{m}$  (0.52 arcsec on sky) slit .
- **Detector readout:** integrate-then-read.
- **Fringe exposure:** Fourier mode (long scan) with dispersion, self fringe-tracking.

The Integrate-Then-Read mode has been described in detail in Sect. 4.3. Below are some details about the modes for the beam combiner, the dispersive element and the fringe exposure.

### 5.1 Acquisition

IRIS (see Sect. 6.4) is normally used for acquisition. If IRIS cannot be used, the MIDI imaging mode should be used for acquisition instead. The imaging mode requires the selection of a spectral filter.

The “N8.7” (N-band short wavelengths) filter normally yields the better signal-to-noise ratio in the exposures obtained from acquisition. Nevertheless, the user has now the possibility to select the filter of his/her choice for the acquisition. This is important if, for example, the target shows strong absorption around 8.7  $\mu\text{m}$ .

The table 1 gives the characteristics of these filters. More data (transmission vs. wavelength plots and ASCII tables) are available from:

<http://www.eso.org/instruments/midi/inst/filters.html>

Name	Central wavelength ( $\mu\text{m}$ )	FWHM ( $\mu\text{m}$ )
Nband	10.34	5.24
SiC	11.79	2.32
N8.7	8.64	1.54
[ArIII]	9.00	0.13
[SIV]	10.46	0.16
[NeII]	12.80	0.21
N11.3	11.28	0.60

Table 1: Characteristics of the MIDI filters.

## 5.2 Beam combination

As already explained in Sect. 4.2.1, the high sensitivity beam combination (HIGH\_SENS) consists in using the R/T=50/50 combining plate alone. In order to obtain photometric information, exposures with one beam only (first A then B) through the beam combiner with the same optical path are recorded, after the fringe observation has been performed.

The SCLPHOT setup uses the same combining plate as HIGH\_SENS, but two beamsplitting plates with R/T  $\approx$  30/70 are inserted in the optical path of each beam before it reaches the combining plate, in order to extract the photometric signal.

## 5.3 Spectral dispersion

Because of the domination of the thermal background in detector frames, it is necessary to spread the incoming light onto a large zone of the detector, to increase the DIT (detector integration time) without saturating the pixels. The sampling time of one fringe has, however, to be adjusted to stay within the atmospheric coherence time at 10  $\mu\text{m}$  (100 ms typically). Respecting this rule, it has been noticed that fringe dispersion on MIDI yields a better sensitivity than undispersed fringes.

Obviously, dispersion in interferometry allows visibility calculation for different spectral channels. In this case, the minimum fringe signal for each spectral channel must be, more or less, equivalent to the limiting correlated magnitude yielding a visibility over the whole N-band (see Sect. 7.1).

The estimated spectral resolution  $\lambda/\Delta\lambda$  of the prism is  $R = 30$  (at  $\lambda = 10.6 \mu\text{m}$ ). The relationship between wavelength (in micron) and detector pixel on MIDI with the prism is given by:

$$\lambda = C_2 X^2 + C_1 X + C_0$$

where  $X$  is the pixel position (1 = left edge column, 320 = right edge column in the displayed image). The coefficients are:

$$\begin{aligned} C_2 &= -0.0001539 \\ C_1 &= 0.009491 \\ C_0 &= 15.451905 \end{aligned}$$

The accuracy of the above formula with these coefficients is  $0.2 \mu\text{m}$ . Future MIDI calibrations should refine these values.

The estimated spectral resolution  $\lambda/\Delta\lambda$  of the grism is  $R = 230$  (at  $\lambda = 10.6 \mu\text{m}$ ). Its  $C_0$ ,  $C_1$ , and  $C_2$  coefficients (see above for definition) are:

$$\begin{aligned} C_2 &= -1.21122 \times 10^{-6} \\ C_1 &= 0.0231223 \\ C_0 &= 7.54423 \end{aligned}$$

The accuracy of the above formula with these coefficients is  $0.1 \mu\text{m}$ . Future MIDI calibrations should refine these values.

In spectral dispersion, a slit is inserted in the intermediate focus inside the cold-optics of MIDI. The width of this slit is  $200 \mu\text{m}$ , which corresponds to  $0.52$  arcsec on sky with the 8-m unit telescopes, and to  $2.29$  arcsec on sky with the 1.8-m auxiliary telescopes.

It is important to notice that the prism and the grism setups use different cold cameras, providing different magnification factors on the detector:

- Prism mode: “Field” camera (as for image acquisition), magnification= 3 pixels per  $\lambda/D$  ( $1 \lambda/D = 0.26$  arcsec on sky).
- Grism mode: “Spectral” anamorphic camera, magnification= 2 pixels per  $\lambda/D$  along the y-axis, and 1 pixel per  $\lambda/D$  along the x-axis (dispersion direction).

## 5.4 Fringe exposure

In P82, two fringe modes are offered: the classical “dispersed-Fourier Mode”, and the new “field/astrometry” mode.

### 5.4.1 Dispersed-Fourier mode

In dispersed-Fourier mode (Fig. 7), fringes are scanned over an OPD that is several  $\bar{\lambda}$  long, to get interferograms (fringe packets) showing the main lobe of the coherence envelope. As the background is strongly correlated between the two interferometric channels, subtraction will cancel the background and enhance the interferometric signal (fringes are shifted by  $\pi$  between the two recombined beams, see Sect. 2.1). The signal obtained for one scan (if the OPD has been compensated to allow fringe detection) is the actual interferogram. Since self

fringe tracking is used, the zero-OPD point is computed in real-time by MIDI for each scan, and then converted into an offset sent to the tracking delay line. In dispersed-Fourier mode, we now systematically use group-delay tracking: the OPD is measured from the position of a fringe peak in the Fourier transform of the frame showing dispersed fringes. Scanning the OPD remains necessary to determine the OPD sign, and also to provide a better quality of the visibility in each spectral channel at data reduction time.

A raw (uncalibrated) visibility estimation requires a few hundred scans.

**The parameters for fringe measurement in dispersed-Fourier mode in P82 are the following (indicative values and subject to minor changes):**

- Dispersion by either prism or grism (see Sect. 5.3).
- One (1) detector frame per OPD sample.
- Five (5) OPD samples for fringe.
- 8 fringes per scan ( $\Rightarrow$  OPD scanning range= 80  $\mu\text{m}$ ).

After completion of the exposure, each interferogram can be individually processed by Fourier transform to yield a raw visibility. The algorithm used for this computation usually involves a Fourier transform of the interferograms, hence the name of this fringe mode.

#### 5.4.2 Field/astrometry mode

This mode is only interesting when it is known that the scientific target consists of a cluster of several not-connected sources in a narrow field-of-view. The aim is therefore to observe several interference fringe-packets, each one corresponding to one of the sources.

We consider a  $\vec{S}$  the pointing vector of a source that is centered in the MIDI field-of-view, and  $\vec{S}'$  the pointing vector of a neighbor source in the MIDI field-of-view (Fig. 8). Both sources will yield fringes separated by the optical path difference:

$$\Delta OPD = \vec{B}(\vec{S} - \vec{S}')$$

where  $\vec{B}$  is the VLTI baseline used by MIDI. In field/astrometry mode, the OPD scanning range is 140  $\mu\text{m}$  (the maximum allowed by the PZT). Since the fringe-packets of the two sources can be observed only simultaneously in a scan if the two sources have a separation angle of the order of  $\Delta OPD/B =$  a fraction of arcsec. Therefore, this mode is reserved to observe very close sources.

The field/astrometry does not use spectral dispersion. The observations can be performed with any of the filters that are used for acquisition (see Sect. 5.1).

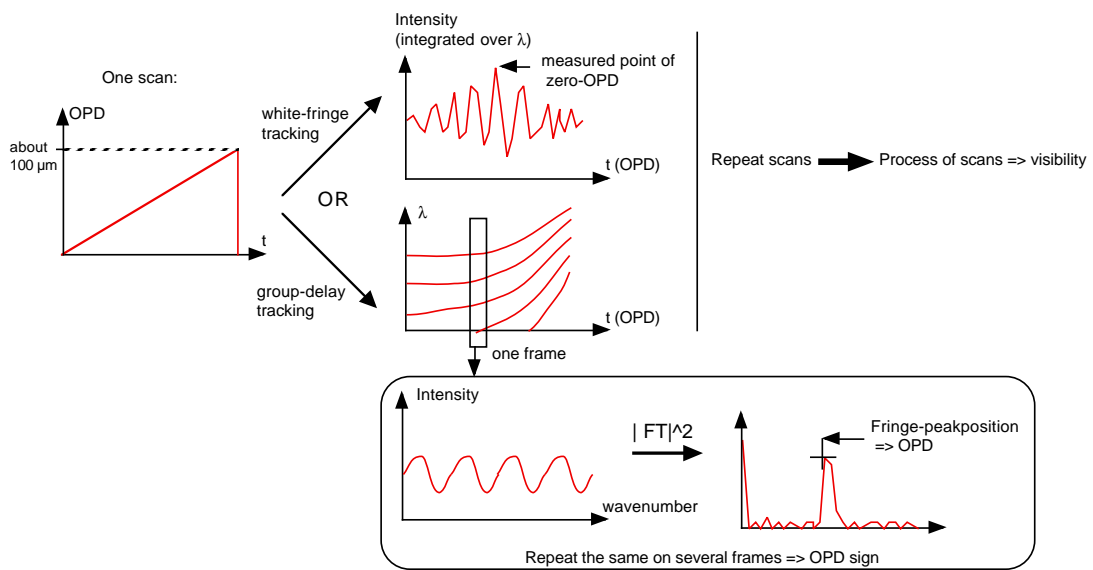


Figure 7: Dispersed-Fourier mode of MIDI. The white-fringe tracking is no longer used for observations.

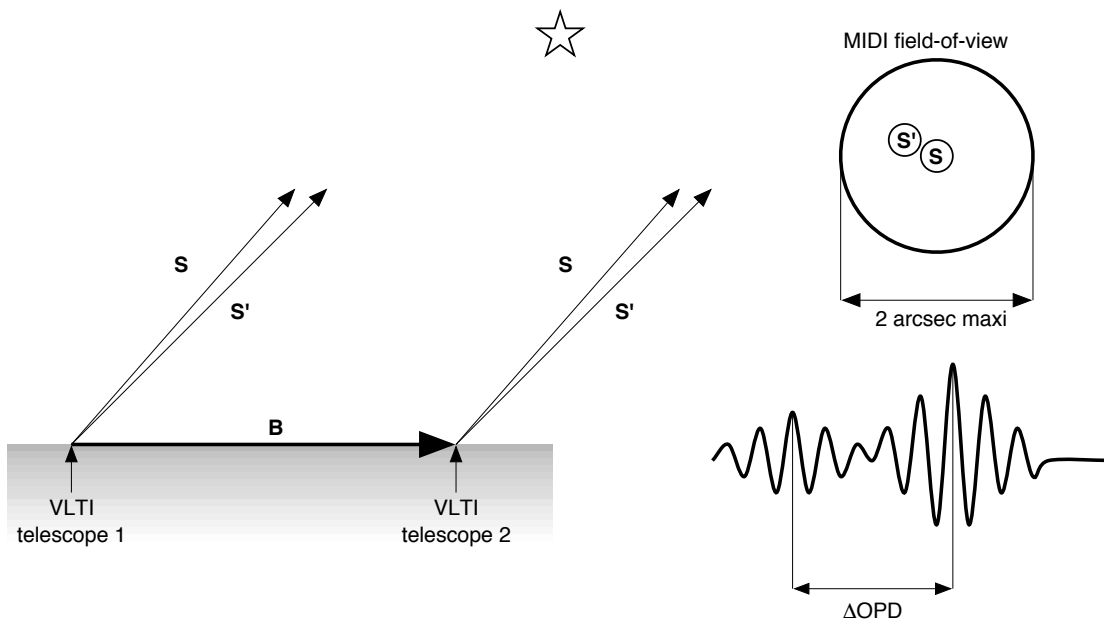


Figure 8: Field/astrometry mode of MIDI.

## 6 THE VLTI ENVIRONMENT IN PERIOD 82

### 6.1 Telescopes and adaptive optics

The available telescopes for MIDI in P82 are the 8-m Unit Telescopes (UTs) of the VLT and the movable 1.8-m Auxiliary Telescopes (ATs).

#### 6.1.1 The Unit Telescopes and MACAO

Each UT is equipped with an adaptive optics system called MACAO. It consists of a Roddier wavefront curvature analyzer using an array of 60 avalanche photodiodes. This analyzer applies a shape correction on the M8 deformable mirror of the UT. The M8 is mounted on a tip-tilt correction stage. In this case, the telescope is tracking in “field stabilization” mode. In this mode, the Nasmyth guide probe camera tracks on a selected guide star (observable within the  $\approx 30$ -arcmin Nasmyth FOV which is centered on the science target) by applying tip-tilt correction to M2. When reaching the limit, the M2 position is offloaded to the alt-az axes of the telescope. The tip-tilt mount of the M8 is offloaded by offsetting the Nasmyth guide probe position, and therefore by offsetting the M2 or the alt-az axes.

The sensitivity of MACAO is  $V = 16$  for a 20% Strehl at  $\lambda = 2.2 \mu\text{m}$ . In practice with MIDI, MACAO can be used with  $V = 17$ . To get diffraction-limited images on MIDI, it is mandatory that MACAO is used. If the target to be observed is fainter than  $V = 17$ , but a suitable guide star exists, it is possible to perform “off-target Coudé guiding”. The guide star must be brighter than  $V = 17$  and closer than 1 arcmin to the target to be observed on MIDI. If  $V > 15$ , there is a risk that Coudé guiding cannot be performed, depending on the off-axis distance and on the sky conditions (seeing,  $\tau_0$ )

If no guide star exists, it is still possible to go through with the target acquisition (in order to ensure beam overlap) by directly offsetting the Nasmyth guide probe from the MIDI observation software, causing a motion of M2 (which is offloaded to the alt-az axes). In this case, only the field stabilization by the Nasmyth probe is enabled, and the image quality on MIDI is usually limited by the seeing. Therefore a lower data quality may be expected. However, this requires an exceptional seeing. In the past, we have noticed that many attempts to observe in SM failed because the seeing was never good enough. Therefore, from P82, **observations without MACAO will be carried out in VM only**. Users are requested to come with an alternative (back-up) observing program, since the conditions to carry out OBs for which MACAO cannot be used are likely to not be encountered.

We guarantee that the MACAO loop is closed, under the following conditions

- Seeing less than 1.5 arcsec.
- Coherence time in visible  $\tau_0$  larger than 1.5 ms.
- Airmass less than 2.
- Distance from the optical axis less than 57.5 arcsec.

#### 6.1.2 The Auxiliary Telescopes and STRAP

Each AT is equipped with the tip-tilt corrector called STRAP. It consists of a avalanche photodiode quadrant which measures the tip-tilt of the incoming wavefront. The measured





Figure 9: A unit telescope (left) and an auxiliary telescope (right).

tip-tilt is compensated by acting on the M6 mobile mirror. When reaching the limit, the M6 position is offloaded to the alt-az axes of the telescope.

The sensitivity of STRAP on the ATs is  $V = 13.5$ . If the target to be observed is fainter than  $V = 13.5$ , it is possible to perform “off-target Coudé guiding”, provided a suitable guide star exists. This guide star must be brighter than  $V = 13.5$  and **closer than 1 arcmin** to the target to be observed on MIDI. If  $V > 12$ , there is a risk that Coudé guiding cannot be performed, depending on the off-axis distance and on the sky conditions (seeing,  $\tau_0$ ).

Note that, unlike the UTs, **the ATs have no possibility of guiding if they cannot guide with the Coudé**. Therefore, it is mandatory to use a suitable Coudé guide star (either the target itself or an off-axis guide star).

### 6.1.3 Chopping

Performing mid-IR observations requires to discriminate the faint stellar signal against a strong and variable background that mostly comes from the sky and optical train thermal emission (see Sec 3.2). The standard technique consists in moving the secondary mirror of the telescope (M2) at a rapid frequency (0.5 Hz typically). The maximum chopping throw of a UT is 30 arcsec, more than needed for the 2-arcsec interferometric field of the VLTI.

Chopping against an empty part of the sky reduces the background signal to zeroth order and normally removes the temporal background variations. An intensity gradient, sometimes strong, remains in the background-subtracted data. It is due to the light paths through the system which are slightly different for the “on” and “off” positions.

Chopping is always used for MIDI image acquisition (to perform the beam overlap), but not during fringe exposure in “HIGH\_SENS” setup. **The power spectrum of the background variations should not affect the fringe visibility down to the offered limiting magnitude (1 Jy in service mode with the prism and HIGH\_SENS beam-combiner for the UTs).**

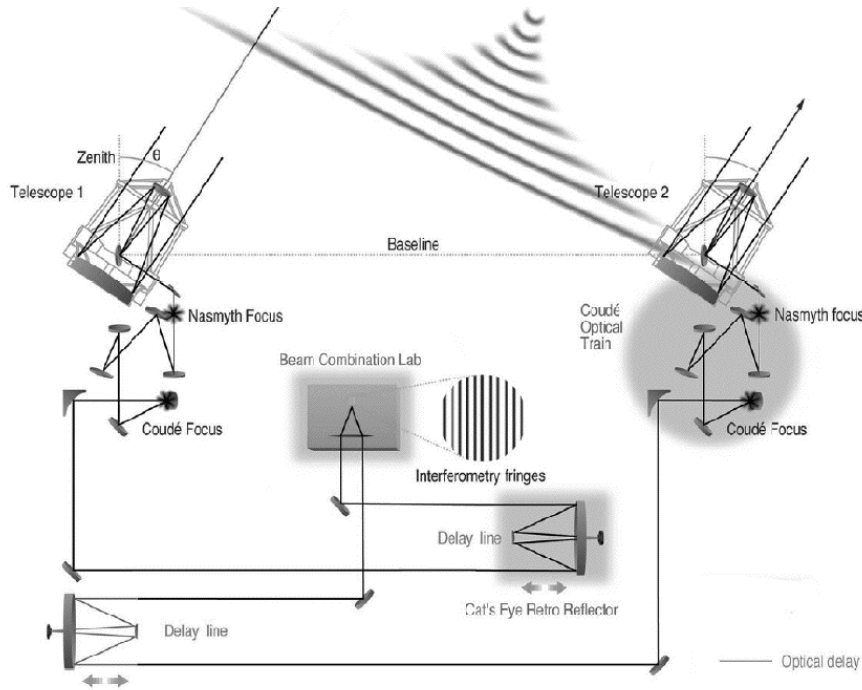


Figure 10: The optical path in the VLTI

## 6.2 Baselines

### 6.2.1 UT Baselines

For P82, **All the four unit telescopes of the VLT are available for MIDI**. The following table gives the characteristics of the possible on-ground baselines ( $E$  is the vector component over the East direction and  $N$  over the North direction):

Name	$E$ (m)	$N$ (m)	On-ground baseline length (m)
UT1-UT2	24.8	50.8	56.5
UT1-UT3	54.8	86.5	102.4
UT1-UT4	113.2	64.3	130.2
UT2-UT3	30	35.7	46.6
UT2-UT4	88.3	13.5	89.3
UT3-UT4	58.3	-22.2	62.4

Note that we cannot guarantee that these six baselines will actually be offered in P82. The final subset of realized baselines will depend on the number of requests for each baseline. Therefore, users might be asked later to switch to the next-best baseline. They can already indicate an alternative baseline in their proposals (as a comment to the interferometric table). For the longest baseline UT1-UT4, there are limitation for the direction of pointing in the sky, related to the mechanical range of the delay-lines. The VisCalc tool (see Sect. 7.3) gives the possible limits.

### 6.2.2 AT baselines

For P82, **A large set of AT baselines is available for MIDI**. To get the exact list, please refer to the webpage:

[http://www.eso.org/paranal/insnews/vlti\\_overview.html](http://www.eso.org/paranal/insnews/vlti_overview.html)

With the commissioning of the variable curvature mirrors (VCMs, see following section) on the different VLTI delay-lines at different times, and in order to have always the VCMs used during observations, the name of the stations that will be used, and therefore the actual names of the baselines may not be the one given in the list. However, the observations will be carried out on equivalent baselines having the same vectors as the ones in the list.

## 6.3 Delay lines

The delay lines are used to compensate the OPD between the two telescopes, from the incoming stellar waveplane to the instrument entrance. Each telescope has a dedicated delay line. One is fixed whereas the other continuously moves in order to compensate OPD for apparent sidereal motion.

The VLTI delay lines are based on a cat's eye optical design featuring a variable curvature mirror (VCM) at its center. The aim of the VCM is to perform a pupil transfer to a desired location, whatever the delay line position. In the case of MIDI, the optimal pupil position is the "cold stop" that is located inside the cryostat after the shutter. The advantages of transferring the pupil are:

- An optimized field of view (1.6 to 5 arcsec with the ATs). Fringes can be obtained from any target within the FOV.
- A reduction of the thermal background related to VLTI optics.

In P82, we guarantee that the VCMs are used for MIDI observations with the **ATs only**.

To compensate OPD drifts due to uncertainty of the array geometry, as well as atmospheric differential piston, position offsets can be applied at high rate to the moving delay line by an OPD controller. The OPD controller receives commands either from the science instrument itself (self fringe-tracking), or from a fringe tracker.

## 6.4 IRIS

IRIS is the infrared field-stabilizer of the VLTI. Its purpose is to perform field-stabilization on the telescopes by measuring the low-frequency tip-tilt from the VLTI laboratory. IRIS guarantees therefore the correct alignment of the beam during the observations. IRIS normally operates in K-band for MIDI operations.

Although the users are requested to give the H-magnitude in the MIDI OBs, this value allows IRIS to work at its best performances, thanks to an adaptive integration time algorithm. An approximation of the H-magnitude can be found from the V-magnitude and the spectral type of the target, using the plot on Fig. 12.

As another advantage, IRIS allows to skip the acquisition by MIDI imaging, reducing considerably the execution overheads. If the target is too faint for IRIS, then the acquisition by MIDI will be executed. Users still have to indicate which MIDI filter has to be used for

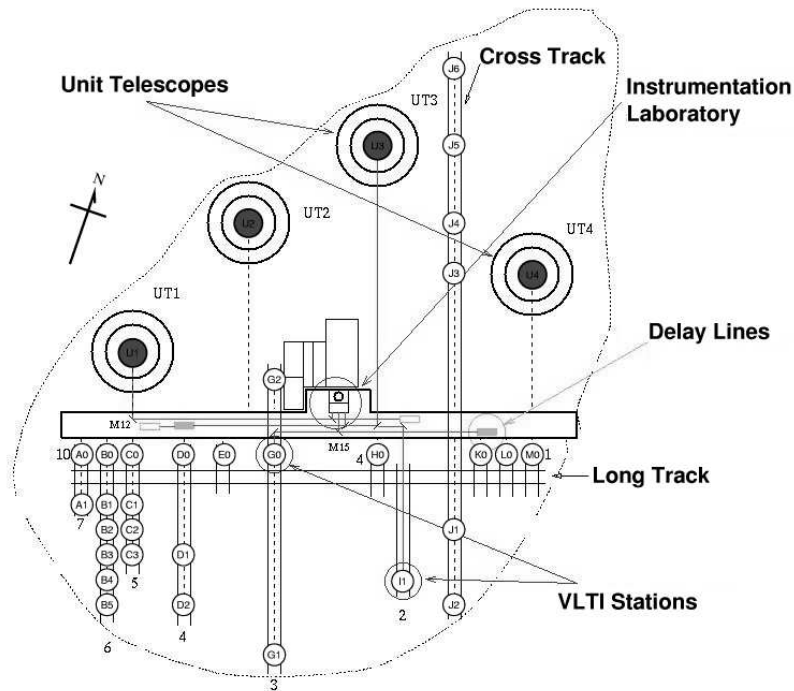


Figure 11: Layout of VLTI telescope locations.

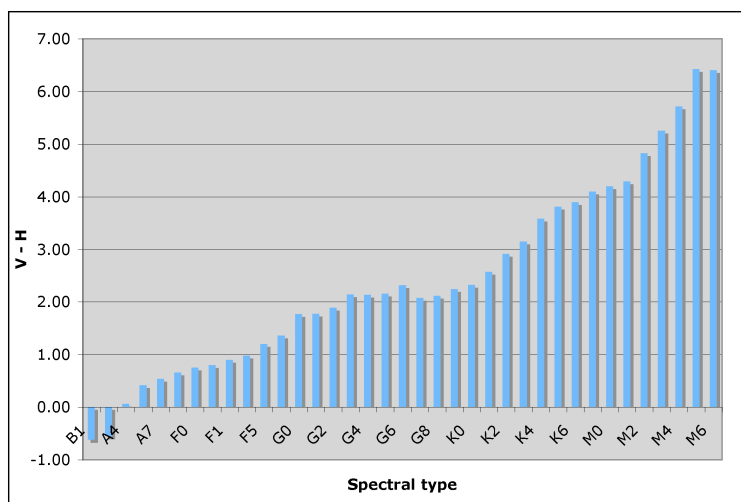


Figure 12: Difference of magnitude between V and H bands, depending on the spectral type.

acquisition, but it does not mean that MIDI acquisition exposures will be taken. Acquisition images are not considered as scientific data and cannot be requested by the users.

## 6.5 FINITO

FINITO is the VLTI fringe tracker. Its purpose is to compensate at high rate the atmospheric differential piston between the two telescopes used by the interferometric instruments, in order to stabilize the fringes. FINITO works in H-band.

During P82, **FINITO can be used with MIDI in VM, in HIGH\_SENS mode, with the ATs only**. The interest of FINITO with MIDI is limited for several reasons:

1. For many targets, the limiting magnitude of MIDI comes from the quality of the photometry exposures.
2. Many MIDI targets are over-resolved in H band. The interest of FINITO would be to observe targets with a high visibility in H, and a low visibility in N. Therefore, FINITO is interesting for very specific MIDI programs (e.g., extended disks around stars).

The performances of FINITO are:

- Limiting magnitude in H: 3
- Limiting magnitude in K (for IRIS fast-guiding): 4
- Limiting visibility in H: 15%

## 6.6 Organization of VLTI observations

**For P82, MIDI is offered in service mode and in visitor mode (see Sect. 1.4).** For the phase-1 of a period, the unique contact point at ESO for the user is the User Support Department (see Sect. 1.5). For the phase-2, USD is still the contact point for service mode, and the Paranal Science Operation department is the contact point for visitor mode ([www.eso.org/observing/p2pp/VisitorMode.html](http://www.eso.org/observing/p2pp/VisitorMode.html)).

**The visitor mode is more likely to be offered for proposals requiring non-standard observation procedures** (like complex structures in the field-of-view of MIDI). The OPC will decide whether a proposal should be observed in SM or VM. As for any other instrument, ESO reserves the right to transfer visitor programs to service and *vice-versa*.

## 7 PHASE-1 PROPOSAL PREPARATION WITH MIDI

Submission of proposals for MIDI should be done through the ESOFORM LaTeX template. It is important to carefully read the following information before submitting a proposal, as well as the ESOFORM user manual. The ESOFORM package can be downloaded from:

<http://www.eso.org/observing/proposals/>

Considering a target which has a scientific interest and for which MIDI could reveal interesting features, the first thing to do is to determine whether this target can be observed with MIDI or not. Several criteria must be taken into account.

### 7.1 Target brightness

The brightness of the target in the N-band will determine whether it is observable at all in self fringe-tracking mode and whether meaningful photometry data can be obtained. **The limiting magnitudes for MIDI observations on unresolved objects in P82 are the following:**

Telescopes	Beam combiner	Dispersion	Limiting mag. (N)	Equivalent in Jy at 12 $\mu\text{m}$
UT	HIGH_SENS	PRISM	4	1
UT	HIGH_SENS	GRISM	2.8	3
UT	SCLPHOT	PRISM	3.2	2
UT	SCLPHOT	GRISM	2	6
AT	HIGH_SENS	PRISM	0.74	20
AT	HIGH_SENS	GRISM	0.31	30
AT	SCLPHOT	PRISM	0.0	40
AT	SCLPHOT	GRISM	-0.44	60

For MIDI in P82, the correlated flux is defined by the uncorrelated flux multiplied by the estimated visibility, i.e. the product brightness  $\times$  visibility. In case of extended objects, which are bright enough to meet the above limits for uncorrelated photometric flux (PF), but have correlated fluxes (CF) below those limits, fringe tracking is still possible to somewhat lower values than noted above:

- Without FINITO:  $\text{CF} = 0.5 \times \text{PF}$
- With FINITO  $\text{CF} = 0.1 \times \text{PF}$

Still, a bright target may be so extended, and therefore has such a low visibility that no fringe tracking is possible on it.

The visual brightness will determine whether MACAO or STRAP can be used on the target or not. As said before, the brightness limit is  $V = 17$  for MACAO on the UTs, and  $V = 13.5$  for STRAP on the ATs.

**The field/astrometry mode is offered for the UTs only, with the limiting correlated magnitude of 5 Jy.** If future commissioning runs prove that this limit can be lowered, waiver for observing fainter targets with this mode will be considered.

Highest achievable precision for calibrated visibilities require observations taken in SCLPHOT mode, with both target and calibrator brighter than 15 Jy with the UTs and 200 Jy with the ATs

## 7.2 Time of observation

It is important to know that in P82, **slots of 60 minutes in service mode, and 90 minutes in visitor mode, per calibrated visibility vs. wavelength curve at a given  $(u, v)$  point, will be attributed, regardless of the correlated magnitude in N-band of the target.** Since the DIT (detector integration time) of MIDI is usually determined by the level of the thermal background illuminating the detector, the user will have no freedom on this parameter. Paranal Science Operation can adjust parameters of fringe exposures for faint objects. The values of these parameters (which are not visible for the user from the templates) are included in the FITS header of the data files that will be delivered to the user after observation.

## 7.3 Geometry

Important parameters of the instrument to be taken into account for the preparation of the observing schedule are the VLTI geometry during observation (the  $(u, v)$  coverage). The selection of the baseline requires the knowledge of both the geometry of the VLTI and of that of the target.

**To assess observability of a target with VLTI, it is mandatory to use the VisCalc software.** The front-end of VisCalc is a comprehensive web-based interface. VisCalc can be used from any browser from the URL:

<http://www.eso.org/observing/etc>

It is important to check that the altitude of the observed object is never below  $30^\circ$ .

Since we had problems in service mode in the past with over-resolved targets (which appeared resolved in imaging mode at the acquisition, or for which no fringes were found), or with low-precision IR coordinates (which could not be seen on MIDI), we encourage the users to collect as much information on their targets as possible, before submitting a MIDI proposal. For instance, a proposal for a pre-imaging study on VISIR (VLT instrument) may help to know more about the feasibility on MIDI.

## 7.4 Guaranteed time observation objects

It is important to check any scientific target against the list of guaranteed time observation (GTO) objects. Only the MIDI consortium is allowed to observe these objects with MIDI, until the end of the guaranteed time period. This guaranteed time period covers the full P82. To make sure that a target has not been reserved already, the list of GTO objects can be downloaded from:

<http://www.eso.org/observing/proposals/gto/index.html>

## 7.5 Calibrator stars

High quality measurements require that the observer minimizes and calibrates the instrumental losses of visibility. To get a correct calibration, the user should use appropriate calibrator stars in terms of target proximity, calibrator magnitude *and* apparent diameter. In the case of MIDI, the calibrator is observed after the science target, using the same templates.

**For each science target, a calibrator star must be provided by the user with the submission of the phase-2 material.** To help the user to select a calibrator, a tool called “CalVin” is provided by ESO. CalVin can be used from any web browser. Like VisCalc, CalVin can be used on the web from:

<http://www.eso.org/observing/etc>

The users have also the possibility to use spectrophotometric calibrators as calibrators of their targets, if they wish to later perform a calibration of the correlated flux. A list of spectrophotometric calibrators (MIDI-consortium calibrators that are also referenced in the ISO catalogs) is available at:

[http://www.eso.org/instruments/midi/tools/spectrophot\\_std.html](http://www.eso.org/instruments/midi/tools/spectrophot_std.html)

## 7.6 Observation constraints

The Moon constraint is irrelevant for mid-IR observations. However, if the Moon is too close to the target (less than 5 deg. typically), the scattered moonlight may prevent MACAO from working correctly. The VLTI astronomers make sure that the OBs in service mode are executed when the Moon is far enough from the targets. In visitor mode, users should carefully schedule their night-time using Moon ephemeris to avoid problems of scattered moonlight.

The seeing condition has no impact on the MIDI image quality: as long as the seeing and the  $\tau_0$  allow MACAO or STRAP correction, the MIDI images are diffraction-limited.

The sky transparency constraint is relevant only in special cases: in HIGH\_SENS mode, thin cloud conditions may cause variations of flux between fringe-track and photometry exposures. Also, if a faint off-axis guide star is used, thin cloud conditions may have impact on the MIDI image quality. On contrary, thin cloud conditions are not a problem in SCI\_PHOT mode if the guide star is brighter than  $V = 15$  (if the UTs are used) or  $V = 12$  (if the ATs are used). The difference between photometric and clear conditions are irrelevant for MIDI operations.



## 8 MIDI OBSERVATIONS

Once a MIDI proposal is accepted by the OPC, it must be set in a form that it can be carried out by Paranal Science Operation. Some knowledge of the observation sequence of MIDI is necessary before tackling phase-2.

### 8.1 Observation sequence

An observation with MIDI in P82 can be split in the several subtasks:

1. Slew telescopes to target position on sky, and slew one of the delay-lines to the expected zero-OPD position. Bring them in “tracking” state (pre-defined sidereal trajectory).
2. Bring telescopes in Nasmyth, then Coudé (MACAO or STRAP) guiding (use of a guide star for field stabilization) if feasible.
3. Adjust telescope positions, so the beams from the target will overlap inside MIDI and be recombined.
4. Search the optical path length (OPL) offset of the tracking delay line yielding fringes on MIDI (actual zero-OPD), by OPD scans at different offsets.
5. Go back to the OPL offset corresponding to zero-OPD, and start to record data of interest: interferograms obtained by OPD scans (fringe exposure).
6. Integrate exposures for photometry, in the same instrument configuration, but with beam A only ; then with beam B only.

Usually the sensitivity is limited by the internal fringe tracking, which has to be performed with integration times that are shorter than the atmospheric coherence time.

#### 8.1.1 Target acquisition

When the operator starts on the instrument an OB received from the OT, the acquisition template begins. The sequence of this template starts by a “preset”: the target coordinates ( $\alpha, \delta$ ) are sent to the telescopes and the delay lines, so they can slew to the position corresponding to the target coordinate at preset time. Once the telescopes are tracking and Coudé-guiding (with MACAO or STRAP), the target can be seen in the FOV of MIDI in imaging mode. To ensure beam interference, the images from both beams must be overlapped. The beam overlap is performed by either:

- Using the IRIS guiding system (see 6.4). IRIS will offset the telescopes to bring the target photocenter onto the reference pixels (defined for the IRIS vs. MIDI alignment) of its detector. IRIS guarantees that the beam overlap is kept by sending corrections to the telescopes. This method will be used as default.

- Using the MIDI acquisition image setup and its associated script that repeats several iterations of the sequence: star photocenter measurement, then offsets calculated and sent to the telescope to bring the star image on a reference pixel of the detector. The loop stops when the error vector for both beams is smaller than a pre-defined threshold (0.8 pixel). This method is now considered as obsolete and is used only if the target is too faint for IRIS.

As stated in Sect.6.1, the user has a possibility to use a guide star for the Coudé systems, different from the target. He/she will have to indicate the coordinates of this star, which, for the UTs (resp. the ATs), should be brighter than  $V = 13.5$  (resp  $V = 17$ ) and within a 1 arcmin (resp. 1 arcmin) radius from the target. If no guide star exists, Coudé guiding will not be used, which may have an impact on the fringe SNR. A seeing constraint has to be indicated.

### 8.1.2 Fringe search

Once beams are overlapped, fringes can be obtained provided VLTI delay line positions yield a zero-OPD ( $\pm 30 \mu\text{m}$ ). In this case, scanning the OPD with the MIDI piezo-mounted mirrors will yield interferograms.

In absence of an external fringe tracker, fringe search for MIDI consists in doing several scans at different delay line position offsets. These offsets are within a range around the expected zero-OPD value (given by an OPD model), and the incremental step of the offset is adjusted for covering the whole fringe search range given by piezo scans. The fringe search is normally executed in “fast” mode: 500- $\mu\text{m}$  OPD steps between two scans, and dispersion using the grism to get the maximum coherence length.

### 8.1.3 Fringe measurement in Fourier mode

Once the delay line offset that yields the zero-OPD is found, a batch of interferograms can be recorded in a series of scans to form an exposure. Group-delay measurements are used to correct the position of the tracking delay-line. If the “SCIPHOT” setup is used, chopping (synchronized with the scans) is performed in order to remove at data reduction time the thermal background from the photometric channels. This does not affect the fringe tracking.

### 8.1.4 Photometry

With the “HIGH\_SENS” setup and in order to compute the fringe visibility from interferograms, it is necessary to measure the flux from each beam through the beam combiner, using the same optical set up as for fringe measurement. Two exposures are therefore taken, with the MIDI shutter at different positions (beam-A open only, then beam-B open only).

Similar exposures are also taken in SCIPHOT, since they can be used to refine the photometry measured in the photometric channels during the fringe exposure. **For P80, the number of frames for the photometry can be adjusted by the user. See the MIDI template manual for details.**

## 8.2 Total sequence timing

As said in Sect. 7.2 for MIDI in P82 the average time to get a calibrated visibility point is 60 minutes in service mode. Hence, the time to complete the above tasks is 30 minutes. This value includes all the overheads. The variable duration of the photometry exposures (set by the user) has a minor impact on the OB execution time.

Visitor mode is usually allocated for targets that require a non-standard acquisition procedure (i.e., very faint target, no Coudé guide star existing, target that is embedded in a complex structure in IR, etc.). In this case, 30 minutes of overheads for the scientific target observation are granted, and the allocated time to get a calibrated visibility is 90 minutes.

## 8.3 The VLT software environment for phase-2

Observations are described by Observing Blocks (OBs). A standard OB consists of:

- A target coordinate set.
- A target acquisition template.
- A set of observation templates for data collection.
- A constraint set.
- A list of intervals of the local sidereal times at which the observations shall be executed.

The templates are the atoms of an OB sequence. They represent the simplest units of an observation and are described extensively in the Template Manual. The P2PP software enables users to create lists of targets. For each target one or several OBs can be created with P2PP by selecting templates and by filling request keyword values (free parameters of the templates) and intervals of the local sidereal times at which the observations shall be executed". The P2PP user manual is available at the ESO website:

<http://www.eso.org/observing/p2pp/#Manual>

For a detailed description of the MIDI templates, please refer to the P82 "MIDI Template Manual". This document will be downloadable, at phase-2 time (around January 2006) from the MIDI webpage at ESO.

## 8.4 Post-observation process

### 8.4.1 Data handling

Data from the MIDI instrument will be stored as FITS binary table files.

Because of the high frame rate of the MIDI detector, the amount of produced data is bulky. One should expect at least 1.2 Gbyte of raw data for each calibrated visibility measurement. To ease data handling, an exposure is split into several 100-Mbyte files (if the exposure is larger than this size), and a file containing the information about the organization of the exposure in multiple files is generated.

### **8.4.2 The pipeline**

Information concerning the pipeline (quick data processor to assess the validity of exposure data) and the data quality control can be found on the web at:

<http://www.eso.org/observing/dfo/quality/>

For the data reduction, there are several IDL packages: MIA (developed by MPIA), EWS (developed by Leiden Observatory), OYSTER (an interface for MIA and EWS). More information can be found at:

<http://www.mpia-hd.mpg.de/MIDISOFT/mia.html>

<http://www.sc.eso.org/~chummel/midi/midi.html>

### **8.4.3 Data distribution**

For any information on the ESO data distribution policy, please check the webpage:

<http://www.eso.org/org/dmd/usg/DataDist.html>

---oOo---